Supplementary materials for: Co-deformation and dynamic annealing effects on the texture development during alpha–beta processing of a model Zr-Nb alloy

Christopher S. Daniel[1*], Alistair Garner[2], Peter D. Honniball[3], Luke Bradley[3], Michael Preuss[2], Philip B. Prangnell[1], João Quinta da Fonseca[1]

[*]Corresponding author, email: christopher.daniel@manchester.ac.uk

[1]Centre for Light Alloy Research and Innovation, The University of Manchester, Manchester, M13 9PL, UK

[2]Materials Performance Centre, The University of Manchester, Manchester, M13 9PL, UK

[3]Rolls-Royce plc, Derby, DE21 7XX, UK

1 Supplementary materials

1.1 Chemical partitioning

Energy dispersive X-ray spectroscopy (EDS) was used to determine partitioning of the alloy elements. This was conducted on an FEI Magellan field emission gun scanning electron microscope (FEG-SEM), at an operating voltage of 30 kV with a working distance 10 mm. The data was recorded at a step size 0.1 μm, with a 0.8 second dwell time, along with the energy range of the EDS detector set at $0 - 20$ keV to capture the K_{α_1} peak of Nb.

1.2 3D EBSD analysis using plasma focused ion beam (PFIB)

To characterise the 3D morphology of the deformed dual-phase microstructure, crystallographic orientations of both the primary α and retained β were measured using 3D electron backscatter diffraction (EBSD). Data was collected using the dual beam Thermo Scientific Helios Xe^+ plasma focused ion-beam SEM (PFIB-SEM). This combines both a Xe^+ source PFIB column with a FEG-SEM in a single vacuum chamber, with automated control of sample movement and FIB milling using Thermo Scientific Auto Slice and View 4 (ASV4) software linked to Oxford Instruments Aztec for EBSD mapping.

For the analysis, a 2D region of interest was initially selected using EBSD, at the centre of the +7Nb alloy sample after rolling at 725°C to 75% reduction. The 2D area in the RD-ND plane (or TD direction) was relocated using the backscatter detector of the Helios microscope, with a surface coating of platinum used to protect the area from subsequent ion damage. A cube volume was then lifted out, by milling a series of trenches either side for full separation [1], using the ion beam operated at 30 kV with a current of 1.3 μA and subsequent lower current cleaning steps. The sample was then mounted on a copper grid using a Pt weld. Standard fiducial marking was applied on the top surface for accurate automated tilting using the ASV4 software. After a further application of Pt of ~ 4 μm thickness to protect the top surface during the automated milling process, slicing was performed using the ion beam operated at 30 kV and 59 nA. Each slice was chosen to remove a material thickness of 0.1 μm across the RD-TD plane (in the ND direction). The current was chosen to deliver a relatively fast slicing time ~ 30 seconds and to improve subsequent EBSD indexing by reducing any material "curtaining" effects. Curtaining was further reduced using a rocking mill, with up to 3° tilt, applied during the milling [2]. For EBSD mapping of each of the individual slices in the RD-TD plane (or ND direction), an electron beam of 20 kV and 22 nA was used, covering an area of 50×50 μm with a step size of 0.15 μm. In this case, 4×4 pixel binning of the EBSD detector optimised both good pattern indexing and relatively fast data acquisition, taking ~ 10 minutes to map each area. The final data set with a total analysis volume of $44 \times 50 \times 50$ μm consisted of 441 individual slices and took ~ 4 days to acquire.

1.3 Data analysis using DREAM.3D and ParaView

The 3D orientation and morphology of both the α and β phases was reconstructed using the DREAM.3D software [3], which was also used to calculate the feature reference misorientation (FRM) and kernel average misorientation (KAM) distributions within the grains. To reconstruct the data, a customise pipeline was developed within DREAM.3D, using a number of data analysis filters and algorithms shown schematically in the *supplementary figures* [3]. A small rotation of $-5°$ was initially applied around the *z*-axis, or ND direction, to align the Euler reference frame with the rolling directions. Image files were then created, including pole figures of the bulk 3D crystallographic orientation data, to check alignment of the Euler reference frame, as well as evaluate the filtered image slices for alignment of the 2D sections. Sections were best aligned with a tolerance set to within 1° of misorientation, for comparing orientations of each sequential 2D EBSD slice. A data point would be classed as mis-indexed and removed if misorientation compared to the 4 nearest neighbours in the 3D data array was greater than 5°. Points with a very low confidence index and high misorientation were also replaced through a neighbour orientation correlation, if two or more

neighbouring cells share a similar orientation. Continuous misorientation boundaries greater than 5° were used to classify grain boundaries and segment the 3D grain features. Features were then assigned phases, feature numbers, along with calculation of average orientation and size. Any grains containing less than 10 cells were removed from the dataset. Within the reconstructed 3D grains, FRM was calculated, as well as a semi-quantitative assessment of energy using the KAM as an indirect measure of microstructural dislocation density. Following a full reconstruction, the final 3D dataset was visualised using the ParaView software [4,5]. Thresholding was used to separate the two phases and analyse the misorientation distribution in different regions of interest, both within a single β-grain, and for comparing different α-grains.

2 Supplementary figures

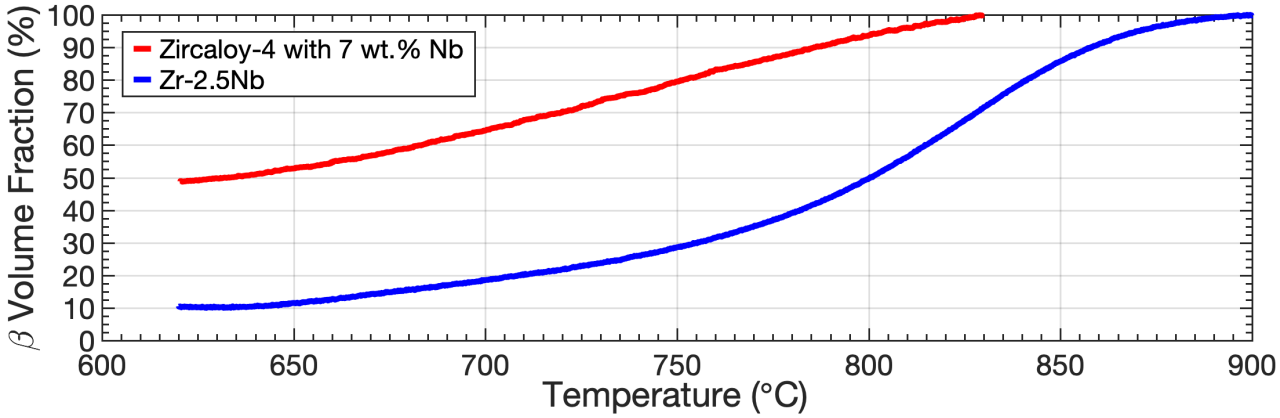

Figure 1: β-phase volume fraction with temperature for the Zircaloy-4 with 7 wt.% Nb alloy, as well as a commercial Zr-2.5Nb alloy [6] for comparison. The transus temperature for the +7Nb alloy was measured using resistivity techniques on an electro-thermal mechanical tester (ETMT) and verified by Rietveld refinement analysis of diffraction spectra data recorded at the Diamond light source (Didcot, UK).

Figure 2: Schematic of the DREAM.3D pipeline [3] used to reconstruct sequential slice EBSD data of the rolled dual-phase Zircaloy-4 + 7 wt.% Nb material, to reproduce the three-dimensional morphology and orientation of primary α grains, as well as the 3D distribution of orientations within the β-matrix.

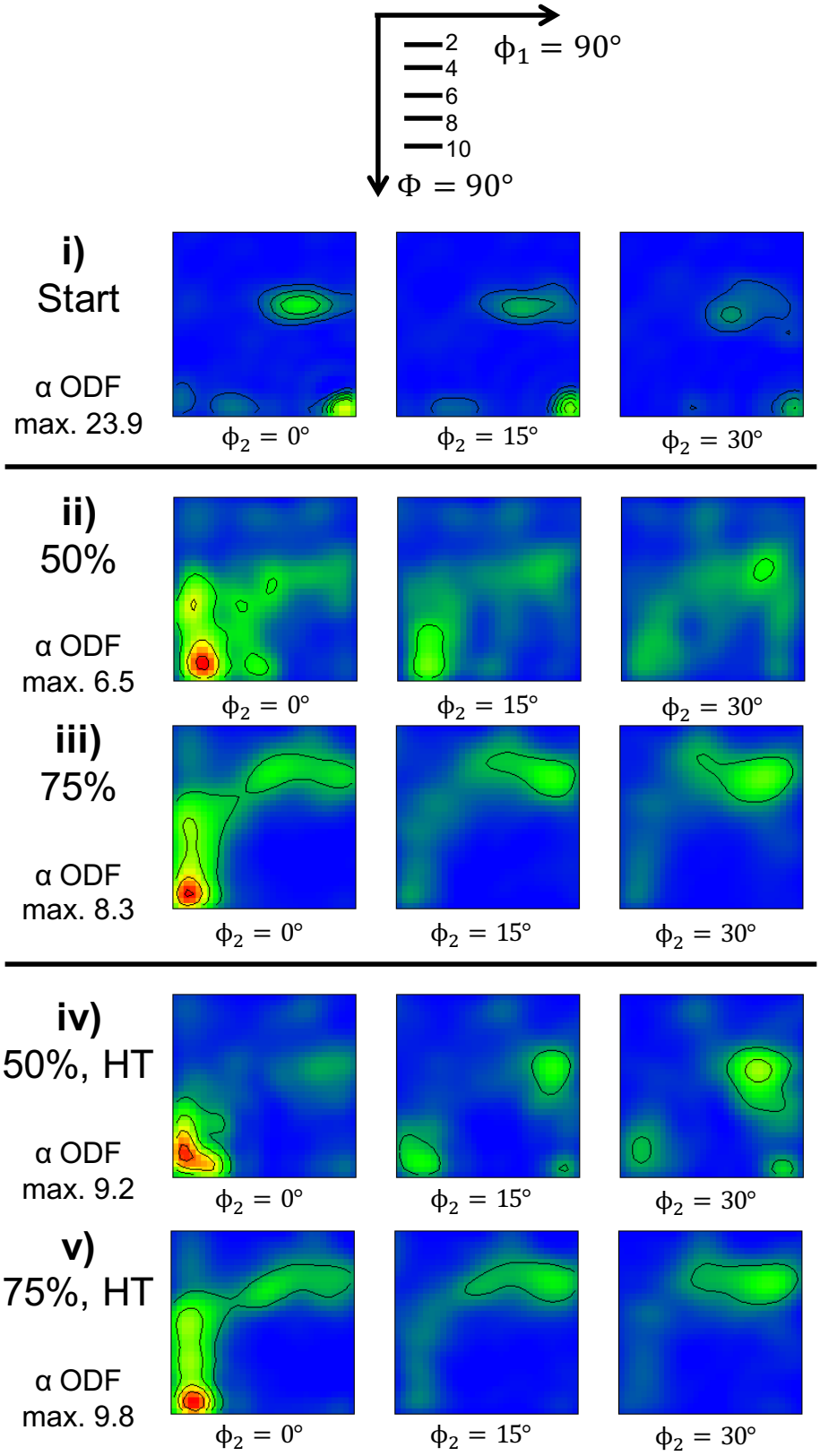

Figure 3: α-phase texture development shown by ODF slices at $\phi_2 = 0°$, $\phi_2 = 15°$ and $\phi_2 = 30°$, showing evolution of (i) starting orientations, after rolling to reductions of (ii) 50% reduction, (iii) 75% reduction, (iv) 50% reduction with annealing HT and (v) 75% reduction with annealing HT. There is initially a very strong starting transformed texture with α basal poles favourably aligned along RD and a maximum at $\phi_1 = 90°$, $\Phi = 90°$ and $\phi_2 = 0°$, followed by the development of a very different $\{11\bar{2}0\}\langle 10\bar{1}0\rangle$ transverse texture component during rolling at $\phi_1 = 0°$, $\Phi = 90°$ and $\phi_2 = 0°$.

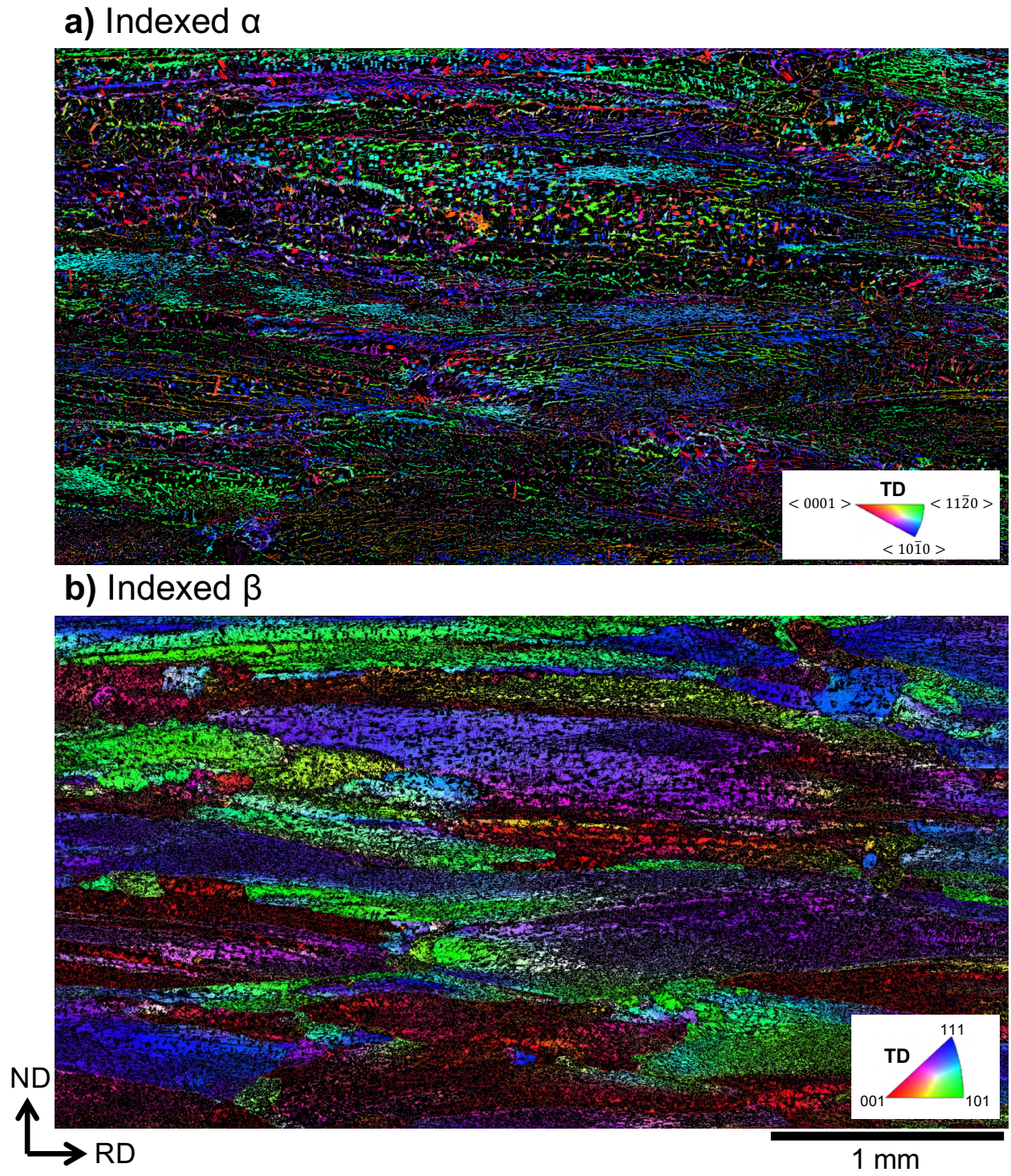

Figure 4: Starting microstructure of the Zircaloy-4 + 7 wt.% Nb alloy, shown by EBSD orientation maps of the (a) indexed α orientations and (b) indexed β orientations, taken with respect to the subsequent rolling directions, in the RD-ND plane (TD direction) and with IPF colouring in TD.

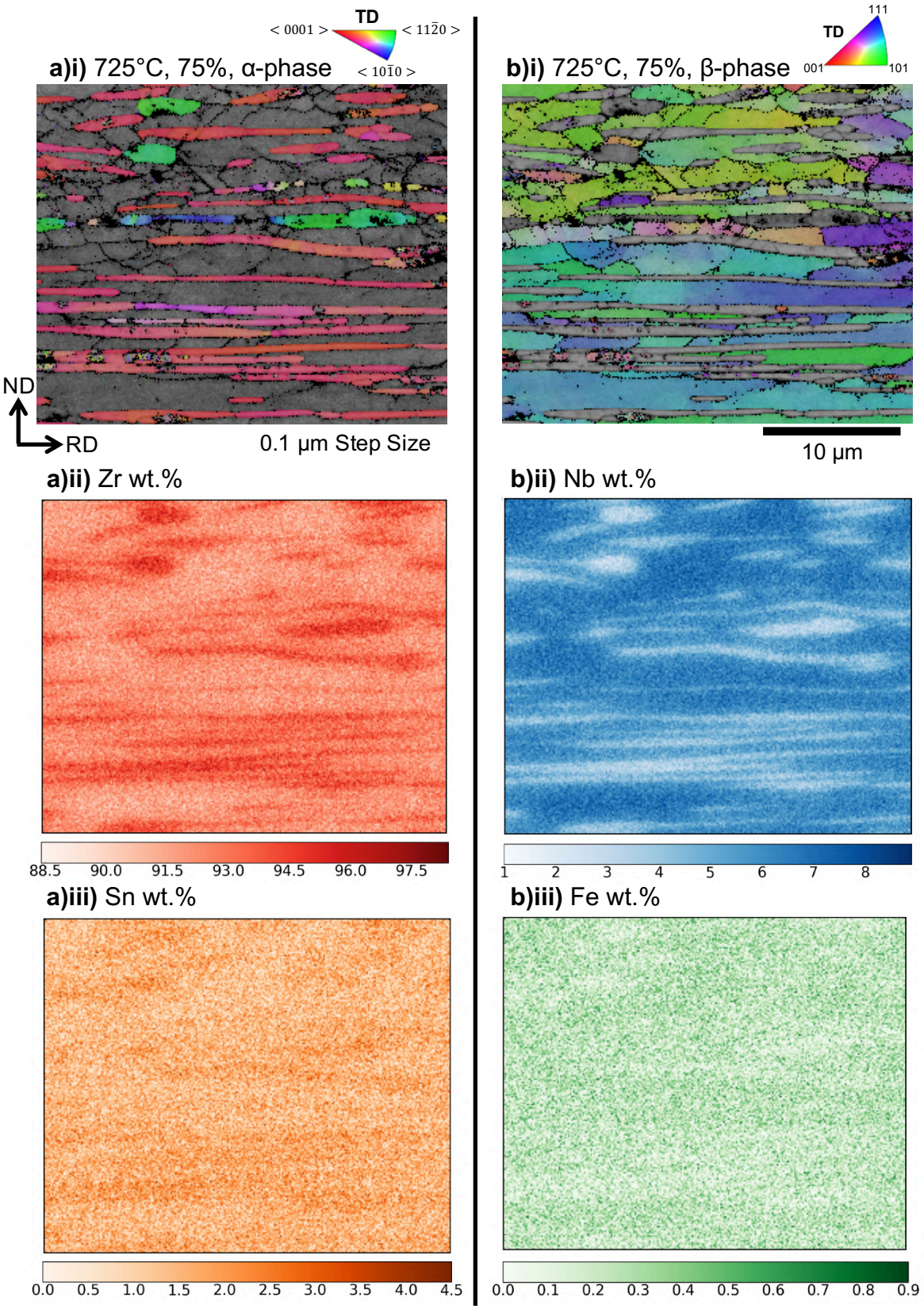

Figure 5: Fine EBSD orientation and EDS chemical maps taken after rolling to 75% reduction, showing (a) indexed α-grains and α-stabilising additions in weight percentage (wt.%) and (b) indexed β orientations and wt.% of β-stabilising additions. Orientation maps in (i) are both shown with IPF colouring in TD. In (a), the amount of (ii) Zr is shown on a scale of 88.4 to 98.4 wt.%, along with the amount of (iii) Sn from 0 to 4.5 wt.%. In (b), the amount of (ii) Nb is shown on a scale of 1 to 8.9 wt.%, along with the amount of (iii) Fe from 0 to 0.9 wt.%. The amount of β-stabilising Cr addition is not shown but did not record any significant element partitioning within a range of 0 to 0.9 wt.%.

References

[1] C. Gillen, A. Garner, A. Plowman, C.P. Race, T. Lowe, C. Jones, K.L. Moore, P. Frankel, Advanced 3D characterisation of iodine induced stress corrosion cracks in zirconium alloys, Mater. Charact. 141 (2018) 348–361. doi:10.1016/j.matchar.2018.04.034.

[2] T.L. Burnett, R. Kelley, B. Winiarski, L. Contreras, M. Daly, A. Gholinia, M.G. Burke, P.J. Withers, Large volume serial section tomography by Xe Plasma FIB dual beam microscopy, Ultramicroscopy. 161 (2016) 119–129. doi:10.1016/j.ultramic.2015.11.001.

[3] M.A. Groeber, M.A. Jackson, DREAM.3D: A Digital Representation Environment for the Analysis of Microstructure in 3D, Integr. Mater. Manuf. Innov. 3 (2014) 5. doi:10.1186/2193-9772-3-5.

[4] J. Ahrens, B. Geveci, C. Law, ParaView: An End-User Tool for Large-Data Visualization, in: Vis. Handb., Elsevier, 2005. doi:10.1016/B978-012387582-2/50038-1.

[5] U. Ayachit, The Paraview Guide: A Parrallel Visualization Application, Kitware, 2015.

[6] C.S. Daniel, P.D. Honniball, L. Bradley, M. Preuss, J. Quinta da Fonseca, A detailed study of texture changes during alpha–beta processing of a zirconium alloy, J. Alloys Compd. 804 (2019) 65–83. doi:10.1016/j.jallcom.2019.06.338.